



Exploration of the binding proteins of perfluorooctane sulfonate by a T7 phage display screen

Yuka Miyano^a, Senko Tsukuda^a, Ippei Sakimoto^b, Ryo Takeuchi^a, Satomi Shimura^a, Noriyuki Takahashi^a, Tomoe Kusayanagi^a, Yoichi Takakusagi^a, Mami Okado^a, Yuki Matsumoto^a, Kaori Takakusagi^a, Toshifumi Takeuchi^a, Shinji Kamisuki^a, Atsuo Nakazaki^c, Keisuke Ohta^b, Masahiko Miura^b, Kouji Kuramochi^{d,*}, Yoshiyuki Mizushima^{e,f}, Susumu Kobayashi^c, Fumio Sugawara^a, Kengo Sakaguchi^a

^a Department of Applied Biological Science, Tokyo University of Science, 2641 Yamazaki, Noda, Chiba 278-8510, Japan

^b Oral Radiation Oncology, Department of Oral Regeneration, Graduate School, Tokyo Medical and Dental University, Yushima, Bunkyo-ku, Tokyo 113-8549, Japan

^c Department of Pharmaceutical Sciences, Tokyo University of Science, 2641 Yamazaki, Noda, Chiba 278-8510, Japan

^d Graduate School of Life and Environmental Sciences, Kyoto Prefectural University, Sakyo-ku, Kyoto 606-8522, Japan

^e Laboratory of Food & Nutritional Sciences, Department of Nutritional Sciences, Kobe-Gakuin University, Nishi-ku, Kobe, Hyogo 651-2180, Japan

^f Cooperative Research Center of Life Sciences, Kobe-Gakuin University, Chuo-ku, Kobe, Hyogo 650-8586, Japan

ARTICLE INFO

Article history:

Received 11 April 2012

Revised 9 May 2012

Accepted 9 May 2012

Available online 15 May 2012

Keywords:

Perfluorooctane sulfonate

Solid-phase synthesis

Phage display

CD14

RELIC

ABSTRACT

Perfluorooctane sulfonate (PFOS) is a pollutant widely found throughout nature and is toxic to animals. We created a PFOS analogue on a polyethylene glycol polyacrylamide copolymer and isolated peptides that preferentially bound the PFOS analogue using a T7 phage display system. Bioinformatic analysis using the FASTAscan program on the RELIC bioinformatics server showed several human proteins that likely bound PFOS. Among them, we confirmed binding between PFOS and a recombinant soluble form of monocyte differentiation antigen CD14 (sCD14) by a surface plasmon biosensor. Furthermore, PFOS inhibited TNF- α production induced by the sCD14 in mouse macrophage RAW264.7 cells.

© 2012 Elsevier Ltd. All rights reserved.

1. Introduction

Perfluorinated alkyl substances (PFAS) have been used in a variety of industrial products such as refrigerants, surfactants, components of paper coatings, fire retardants, adhesives, cosmetics and insecticides.¹ While they have unique and useful properties such as chemical inertness, thermal stability, low surface energy and amphiphilic character, PFAS are difficult to break down in nature and thus bioaccumulate.

Previous reports describe the wide distribution of perfluorooctane sulfonate (PFOS) in the environment and its impact on a range of biological events, although little is known about the detailed mechanisms underlying its physiological activity (Fig. 1). PFOS has been demonstrated to induce liver cancer in rats and mice by activation of the peroxisome proliferator-activated receptor α (PPAR α) that leads to peroxisome proliferation.^{2–5} However, recent reports show that PFOS-induced toxicity is independent of PPAR α activation.^{6–8} PFOS affects lipid metabolism,^{3,9–11} blocks gap

junction intercellular communication both in vitro and in vivo,¹² and increases production of reactive oxygen species in cultured cells including hepatoma Hep G2 cells¹³ and human umbilical vein endothelial cells (HUVECs).¹⁴ In addition, PFOS substantially inhibits 3 β -hydroxysteroid dehydrogenase, 17 β -hydroxysteroid dehydrogenase^{3,15} and 11 β -hydroxysteroid dehydrogenase^{2,16}. Our group previously found that PFOS was a potent inhibitor of mammalian DNA polymerases (pol) α and β , and human terminal deoxynucleotidyl transferase.¹⁷ Unlike classic fatty acid inhibitors against mammalian DNA polymerases (many of which selectively inhibit binding of the N-terminal 8 kDa domain of pol β to a DNA template), PFOS inhibits primer extension catalyzed by the 31 kDa domain of pol β .

Phage display is a powerful system which can identify target proteins of small molecules,^{18–23} and also determine the binding

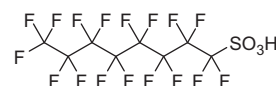


Figure 1. Structure of perfluorooctanesulfonic acid.

* Corresponding author.

E-mail address: kuramochi@kpu.ac.jp (K. Kuramochi).

sites of target proteins for small compounds.^{24–26} Analysis of affinity-selected peptides from phage libraries by RELIC, a bioinformatics server for combinatorial peptide analysis, is anticipated to become a powerful tool for identifying both binding proteins of small molecules and protein–ligand interaction sites.^{27–29} We previously illustrated the potential of polyethylene glycol polyacrylamide copolymer (PEGA) resin as an affinity matrix for phage display screening.³⁰ PEGA resin, which is generally used for solid-phase synthesis, has several attractive features including chemical stability, high coupling capacity and favorable swelling in both organic solvents and aqueous media.³¹ Thus, both the synthesis of ligand and the subsequent ligand affinity selection can be achieved on the same PEGA resin.

In this study, we synthesized a PFOS-analogue-immobilized PEGA resin and screened for peptides that bind to PFOS using a T7 phage display screen.

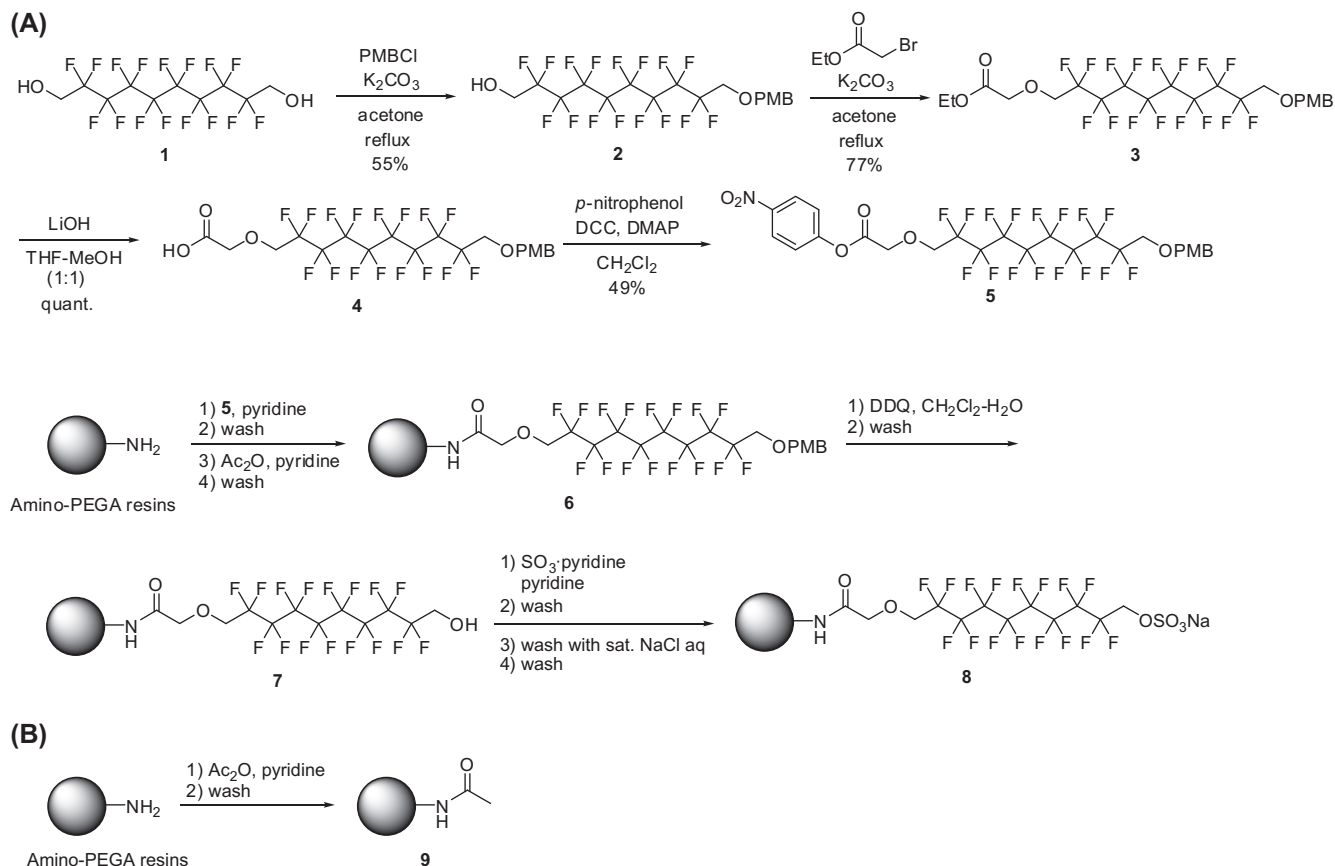
2. Results

Peptides with high affinity to PFOS were searched using T7 phage display with a PEGA-supported PFOS analogue. Since it is difficult to immobilize PFOS on affinity supports directly and construct the sulfonate moiety of PFOS on PEGA resin, 1*H*,1*H*-perfluorononyl sulfate moiety was synthesized on the surface of PEGA resin (Scheme 1A). The synthesis was started from 2,2,3,3,4,4,5,5,6,6,7,7,8,8,9,9-hexadecafluoro-1,10-decanediol (**1**). One hydroxyl group was protected as its *p*-methoxybenzyl ether. Treatment of **2** with ethyl bromoacetate in the presence of potassium carbonate gave **3**. Hydrolysis of the ethyl ester with lithium hydroxide afforded carboxylic acid **4**, which was subsequently converted into

p-nitrophenyl ester **5** for immobilization on amino-PEGA resin. After immobilization of **5** onto the resin, the residual amino groups were blocked with acetic anhydride. The removal of the *p*-methoxybenzyl group on resin **6** with DDQ in dichloromethane–water (10:1) gave PEGA-supported 1*H*,1*H*-perfluorononyl sulfate **7**. Finally, treatment of **7** with SO₃·pyridine, followed by ion exchange with saturated NaCl solution gave a PEGA-supported PFOS analogue **8**. In addition, a control resin **9** by acetylation of amino-PEGA resin was prepared (Scheme 1B).

A library displaying random peptides on phage particles was incubated with the PEGA-supported PFOS analogue **8** or the control resin **9**. After removal of unbound phage clones, the bound phage particles were eluted and amplified in *Escherichia coli*. The recovered phages were subjected to the next round of selection. In the third and fourth rounds of selection, approximately 3- to 4-fold more phage particles were recovered from **8** than from **9** (Fig. 2). Among phages eluted from **8** in the fourth round of selection, 32 randomly picked clones were sequenced (Table 1). We next sought to explore PFOS-binding proteins by bioinformatically analyzing a pool of amino acid sequences displayed by phage particles that bound to **8**. The FASTAscan program developed by the RELIC bioinformatics ranked proteins in descending order of score that is calculated from sequence similarity between queried peptides and human gene products.^{27,32} Among nine proteins with the highest score (Table 2), we focus on monocyte differentiation antigen CD14.

A physical interaction between PFOS and CD14 was analyzed using a surface plasmon resonance biosensor instrument, Biacore3000 (Fig. 3). A soluble form of recombinant CD14 that lacked the C-terminal 21 amino acids (sCD14 [1–335]) was immobilized



Scheme 1. Synthesis of PFOS analog-immobilized PEGA resin **8** (A) and acetylated control resin **9** (B).

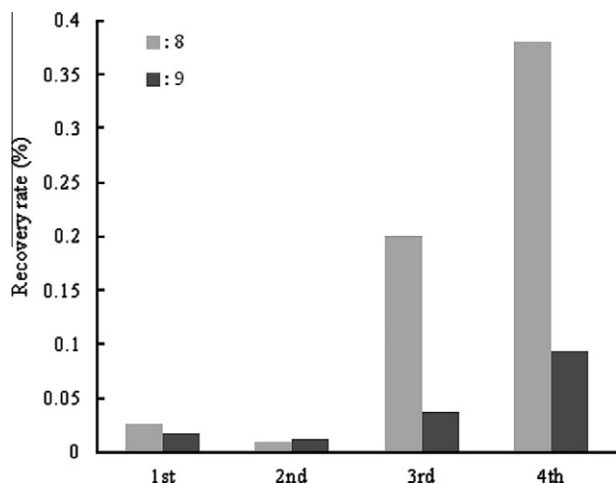


Figure 2. Recovery rate of phage particles bound to **8** and **9** after each round of biopanning. The phage random library was applied to **8** or **9**. After removal of unbound phage particles, bound phage particles were eluted and amplified by infection of *E. coli*. The resulting phage particles were used in the next round of selection. At each round, the recovery rates of the eluted phage particles to the input phage particles from the resins were calculated.

Table 1

Amino acid sequence of peptides displayed on the phage particle after the biopanning using PEGA-supported PFOS analogue (**8**)

Phage clone	Sequence ^a	Frequency ^b
1	PVSPFTCDLGARTSP	12/32
2	VRDVFSVCGGVSSCHESLRPHSSN	6/32
3 ^c	PAGISRELVDKLAALAE	3/32
4	LSRAGSLGSLRHA	2/32
5	SCTSYAGSLNFSL	2/32
6	LHSFDFVTNVSVFV	1/32
7	SCTSYVGSILNFSL	1/32
8	PVLSPPFDAGLVKACGRTRVTS	1/32
9	SRFECNLGACPVRAC	1/32
10	FGCTLPIAVCRVADE	1/32
11	GCLSFITYGYPWWLPR	1/32

^a Amino acid sequences were determined from DNA sequences of the insert DNA.

^b Frequency is the number of sequences among the total phage clones selected.

^c This phage clone does not contain the inserted DNA fragment.

Table 2

List of human proteins with high similarity to the selected peptides^a

Score ^b	Protein
777.78	Protocadherin Fat3
678.85	Monocyte differentiation antigen CD14
647.31	Olfactory receptor 4K17
627.60	Adiponutrin
622.22	Integrin alpha-M precursor
612.54	Splice isoform of prostaglandin E2 receptor
595.34	Chondroitin sulfate synthase 1
574.55	Retinoblastoma-like protein 2
561.29	Cadherin 4

^a The candidates for PFOS-binding proteins were obtained by analysis of selected peptides using the FASTAscan program from the Receptor Ligand Contacts (RELIC).

^b Scores are generated by calculating the similarity between all peptides and each segment of the protein sequence.

on a CM5 sensor chip by the amine coupling reaction.^{33,34} Several concentrations of PFOS were injected over the sCD14 [1–335]. As shown in Figure 3, negative sensorgrams were observed. The negative response was enhanced at increasing concentrations of PFOS, confirming a specific interaction between PFOS and sCD14 [1–335]. The negative sensorgrams might be explained by conformation changes in the sCD14 [1–335] bound to PFOS, as described in

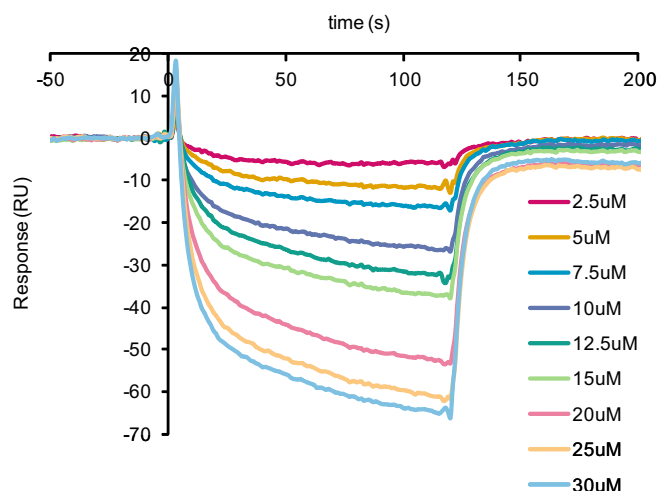


Figure 3. SPR analysis of the binding between PFOS and a recombinant soluble CD14 (sCD14 [1–335]). sCD14 [1–335] was immobilized on a CM5 sensor chip. PFOS samples were injected over the immobilized sCD14 [1–335]. Response units (RU) were calculated by subtracting the background response measured in the control flow cell from the response in each sample flow cell. Binding of various concentrations of PFOS to the sCD14 was analyzed. The concentrations of PFOS were 2.5, 5.0, 7.5, 10.0, 12.5, 15, 20, 25 and 30 μ M from top to bottom. Kinetic studies were performed using the BIA evaluation software.

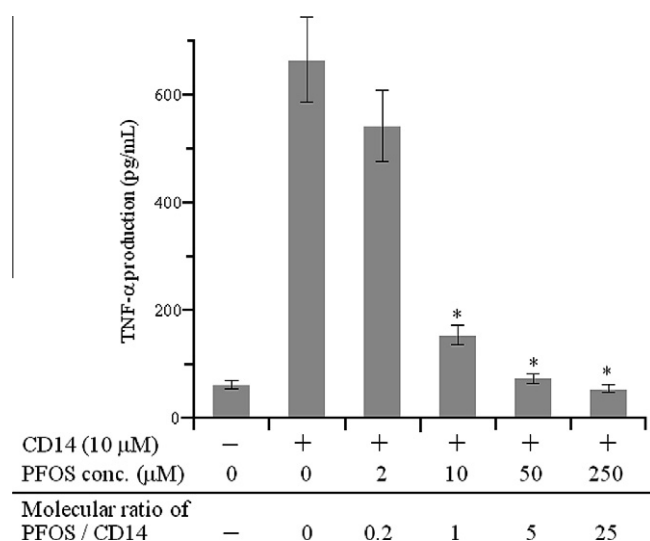


Figure 4. Inhibitory effects of PFOS on CD14-induced production of TNF- α in the mouse macrophage cell line RAW264.7. The indicated molecular ratios of PFOS and CD14 protein were pre-incubated for 10 min at room temperature, and the mixture was incubated with the cells for 24 h. The TNF- α concentration in the cell medium was measured by ELISA. Data represent means \pm SD ($n = 4$). *, $P < 0.01$ versus untreated control (student's t -test).

previous reports.^{35–37} The apparent dissociation constant value for this binding was determined to be 5.83×10^{-5} M.

Next, we investigated whether PFOS can inhibit the sCD14 function in mouse macrophage RAW264.7 cells. As shown in Figure 4, the sCD14 [1–335] significantly induced TNF- α production in the cultured cells (10 μ M of CD14-evoked TNF- α level, 665.0 pg/mL). This CD14 stimulation was inhibited by the pre-incubation of CD14 protein and PFOS. When the molecular ratio of PFOS and CD14 was more than 1, the TNF- α production of the cells was inhibited. In cultured macrophage RAW264.7 cells, PFOS was not cytotoxic at 250 μ M (data not shown); therefore, the LD₅₀ value was >250 μ M. These results suggest that PFOS will directly bind

sCD14 and prevent TNF- α production induced by CD14 in macrophages.

3. Discussion

Here, we employed a combination of a T7 phage display technology and PFOS coupled to PEGA resin in order to identify amino-acid sequences bound to the small ligand. Use of PEGA resin facilitates preparation of a hydrophobic compound-immobilized matrix as the resin can be used during both solid-phase synthesis of the ligand in organic solution and in vitro selection of phage particles displaying oligopeptides in aqueous solution. The screen was successfully achieved because the recovery rate of the eluted phage particles from **8** against input phage particles increased with each round of biopanning.

Analysis of selected peptides using the FASTAscan program from RELIC provides candidates of PFOS-binding proteins. Among the candidate binding proteins, PFOS interacts with sCD14 [1–335] with an apparent dissociation constant of 5.83×10^{-5} M by SPR analyses. CD14 is known to exist either in a glycosylphosphatidylinositol anchored form on the surface of cells (membrane CD14, mCD14) or in a soluble form in blood (sCD14).³⁸ Previous studies showed that sCD14 binds lipopolysaccharide (LPS) in the absence of lipopolysaccharide binding protein (LBP).^{39,40} The LPS–sCD14 complexes are considered to be an important intermediate in the inflammatory responses of leukocytes to LPS.⁴¹

PFOS has been reported to alter inflammatory responses and production of cytokines in both PPAR- α dependent and independent manners.^{8,42,43} Recent studies showed that the immunotoxicity of PFOS could be explained by its inhibitory effects on LPS-induced I- κ B degradation.^{44,45} We found that pre-incubation of PFOS and sCD14 [1–335] inhibited TNF- α production induced by the sCD14 in RAW264.7 cells. Since the critical micelle concentration of potassium perfluorooctane sulfonate is reported to be 8 mM,⁴⁶ PFOS would not form micelles at the concentration used in this study and act as a surfactant to sCD14 [1–335]. Taken together with our SPR analyses, these results suggest that PFOS will directly bind sCD14 and inhibit the function of sCD14, which might be another mechanism for the immunotoxicity of PFOS.

In conclusion, we identified CD14 as a binding protein of PFOS by a combination of solid-phase synthesis of a ligand with a T7 phage display screen. Although further study is required to elucidate the binding site of PFOS within CD14 as well as detailed mode of action of PFOS, our results suggested that PFOS might cause the immunotoxicity by impeding the function of CD14.

4. Experimental procedure

4.1. General methods for synthesis of a PEGA-supported PFOS-analogue (**8**) and control resin (**9**)

All reagents were obtained from commercial sources and used without further purification. Analytical thin-layer chromatography was performed on Silica Gel 60 F₂₅₄ plates (Merck, Darmstadt, Germany). Flash chromatography was carried out on PSQ 100B (Fuji Silysia Co., Japan). ¹H NMR spectra were recorded on a Bruker 600 MHz spectrometer (Avance DRX-600) using a CDCl₃ solution, unless otherwise noted. Chemical shifts are expressed in δ (ppm) relative to Me₄Si and coupling constants (*J*) are expressed in hertz. Melting point (mp) data were determined with a Yanaco MP-3S instrument and are uncorrected. Infrared (IR) spectra were recorded on a Jasco FT/IR-410 spectrometer, using NaCl (neat) or KBr pellet (solid). Mass spectra (MS) were obtained on an Applied Biosystems mass spectrometer (API QSTAR pulsar i) under high-resolution conditions.

4.2. Preparation of 2,2,3,3,4,4,5,5,6,6,7,7,8,8,9,9-hexadecafluoro-1-(*p*-methoxybenzyloxy)decanol (**2**)

A solution of 1*H*,1*H*,10*H*,10*H*-perfluorodecane-1,10-diol (597 mg, 1.29 mmol), *p*-methoxybenzyl chloride (140 μ L, 1.03 mmol) and potassium carbonate (536 mg, 3.88 mmol) in acetone (3 mL) was refluxed for 72 h. The reaction was then quenched by the addition of water and diluted with EtOAc. The layers were separated, the organic layer was washed with brine, dried (Na₂SO₄) and concentrated. The residue was purified by silica gel chromatography (hexane/EtOAc = 3:1) to yield **2** (331 mg, 55%) as white solid. Mp = 49.1–51.1 °C. ¹H NMR (270 MHz, CDCl₃) δ 7.27 (2H, d, *J* = 8.6 Hz), 6.90 (2H, d, *J* = 8.6 Hz), 4.60 (2H, s), 4.10 (2H, m), 3.90 (2H, t, *J* = 13.9 Hz), 3.82 (3H, s), 1.93 (1H, br m). IR (KBr) 3394, 2961, 2939, 2870, 2844, 1615, 1518, 1463, 1382, 1303, 1252, 1199, 1146, 1029, 973, 819 cm⁻¹. HRMS (ESI): calcd for C₁₈H₁₄O₃F₁₆Na ([M+Na]⁺) 605.0579, found 605.0582.

4.3. Preparation of ethyl {2,2,3,3,4,4,5,5,6,6,7,7,8,8,9,9-hexadecafluoro-10-(*p*-methoxybenzyloxy)decanyloxy}acetate (**3**)

A solution of **2** (331 mg, 0.57 mmol), ethyl bromoacetate (95 μ L, 0.85 mmol) and potassium carbonate (393 mg, 2.84 mmol) in acetone (5 mL) was stirred at room temperature for 18 h and then refluxed for 6 h. Ethyl bromoacetate (60 μ L, 0.54 mmol) was added to the mixture, the resulting mixture was refluxed for 15 h. Since the reaction was not completed, additional ethyl bromoacetate (120 μ L, 1.08 mmol) was added to the mixture. After the mixture was refluxed for 5 h, the reaction was quenched by the addition of water. The resulting mixture was diluted with EtOAc. The layers were separated, the organic layer was washed with brine, dried (Na₂SO₄) and concentrated. The residue was purified by silica gel chromatography (hexane/EtOAc = 6:1) to yield **3** (293 mg, 77%) as colorless oil. ¹H NMR (270 MHz, CDCl₃) δ 7.26 (2H, d, *J* = 8.4 Hz), 6.90 (2H, d, *J* = 8.4 Hz), 4.61 (2H, s), 4.24 (2H, q, *J* = 7.1 Hz), 4.23 (2H, s), 4.11 (2H, t, *J* = 13.8 Hz), 3.89 (2H, t, *J* = 13.9 Hz), 3.82 (3H, s), 1.29 (3H, t, *J* = 7.1 Hz). IR (KBr) 2943, 2850, 1754, 1614, 1588, 1514, 1465, 1377, 1213, 1146, 1035, 960, 823 cm⁻¹. HRMS (ESI): calcd for C₂₂H₂₀O₅F₁₆Na ([M+Na]⁺) 691.0947, found 691.0925.

4.4. Preparation of {2,2,3,3,4,4,5,5,6,6,7,7,8,8,9,9-hexadecafluoro-10-(*p*-methoxybenzyloxy)decanyloxy}acetic acid (**4**)

A solution of **3** (159 mg, 0.24 mmol) and 1 M aqueous LiOH (1.0 mL, 1.00 mmol) in THF (1.5 mL) and MeOH (1.5 mL) was stirred at room temperature for 3 h. The mixture was then acidified by the addition of 1 M HCl and diluted with EtOAc. The layers were separated and the aqueous layer extracted twice with EtOAc. The combined organic layer was washed with brine, dried (Na₂SO₄) and concentrated to give **4** (242.3 mg, quant) as a colorless solid. Mp = 77.5–78.5 °C. ¹H NMR (270 MHz, CDCl₃) δ 7.26 (2H, d, *J* = 8.6 Hz), 6.90 (2H, d, *J* = 8.6 Hz), 4.61 (2H, s), 4.32 (2H, s), 4.14 (2H, t, *J* = 13.6 Hz), 3.89 (2H, t, *J* = 13.7 Hz), 3.82 (3H, s). IR (KBr) 3480, 2994, 2961, 2937, 2838, 1730, 1614, 1588, 1518, 1459, 1367, 1315, 1251, 1214, 1139, 1032, 995, 975, 951, 828 cm⁻¹. HRMS (ESI): calcd for C₂₀H₁₆O₅F₁₆Na ([M+Na]⁺) 663.0634, found 663.0614.

4.5. Preparation of *p*-nitrophenyl {2,2,3,3,4,4,5,5,6,6,7,7,8,8,9,9-hexadecafluoro-10-(*p*-methoxybenzyloxy)decanyloxy}acetate (**5**)

To a solution of **4** (154.5 mg, 0.24 mmol) and *p*-nitrophenol (67.8 mg, 0.48 mmol) in CH₂Cl₂ (4 mL) was added *N,N*-

dicyclohexylcarbodiimide (102 mg, 0.49 mmol) followed by 4-dimethylaminopyridine (31.2 mg, 2.6 mmol). The mixture was stirred at room temperature for 5 h. The reaction was quenched by the addition of water. The resulting mixture was diluted with EtOAc. The layers were separated, the organic layer was washed with brine, dried (Na_2SO_4) and concentrated. The residue was purified by silica gel chromatography (hexane/EtOAc = 3.5:1) to yield **5** (78 mg, 49%) as yellow solid. Mp = 41.5–42.5 °C. ^1H NMR (270 MHz, CDCl_3) δ 8.30 (2H, d, J = 9.1 Hz), 7.34 (2H, d, J = 9.1 Hz), 7.26 (2H, d, J = 8.6 Hz), 6.90 (2H, d, J = 8.6 Hz), 4.61 (2H, s), 4.55 (2H, s), 4.21 (2H, t, J = 13.5 Hz), 3.90 (2H, t, J = 13.9 Hz), 3.82 (3H, s). IR (KBr) 3006, 2938, 2842, 1775, 1618, 1592, 1537, 1518, 1486, 1459, 1351, 1250, 1207, 1145, 1031, 966, 920, 859, 822 cm^{-1} . HRMS (ESI): calcd for $\text{C}_{26}\text{H}_{19}\text{NO}_7\text{F}_{16}\text{Na}$ ($[\text{M}+\text{Na}]^+$) 784.0798, found 784.0772.

4.6. Preparation of resin 6

Amino-PEGA resin (0.42 g, 0.021 mmol) was washed with CHCl_3 ($\times 3$) and pyridine ($\times 3$) and swollen in pyridine (2 mL). To the suspension of the resin was added **5** (32 mg, 0.042 mmol), and the suspension stirred at room temperature for three days. Then the suspension was filtered and washed with CHCl_3 three times. The resulting resin **6** was dried and used for the next reaction. The filtrate was concentrated, and the residue was purified by silica gel chromatography (hexane/EtOAc = 1:1) to give *p*-nitrophenol (4.5 mg, 77% from **5**) and the recovered **5** (6.4 mg).

4.7. Preparation of resin 7

Resin **6** was swollen in CH_2Cl_2 – H_2O (10:1; 4.4 mL). To the suspension of the resin was added 2,3-dichloro-5,6-dicyano-*p*-benzoquinone (17.1 mg, 0.021 mmol), and the mixture was stirred at room temperature for 24 h. Then the suspension was filtered and washed with CHCl_3 three times, MeOH – H_2O three times, and CHCl_3 twice. The resulting resin **7** was dried and used for the next reaction. The organic layer was separated from the filtrate. The organic layer was washed with saturated NaHCO_3 , brine, dried (Na_2SO_4) and concentrated. The residue was purified by preparative TLC (hexane/EtOAc = 1:1) to give anisaldehyde (1.8 mg, 80% calculated from amino-PEGA resin).

4.8. Preparation of resin 8

Resin **7** was swollen in pyridine (4 mL). To the suspension of the resin was added sulfur trioxide pyridine complex (12.0 mg, 0.075 mmol), and the mixture was stirred at room temperature for 24 h. Then the suspension was filtered and washed with CHCl_3 three times, MeOH three times, MeOH – H_2O three times, H_2O twice, saturated aqueous solution of NaCl and H_2O twice. The resulting resin **7** was dried and used for affinity selection.

4.9. Preparation of resin 9

Amino-PEGA resin (1.0 g) was washed with CHCl_3 twice and pyridine twice and swollen in pyridine (5.0 mL). To the suspension of the resin was added Ac_2O (5.0 mL), and the suspension was stirred at room temperature for 3 h. Then the suspension was filtered and washed with CHCl_3 three times, MeOH three times, and CHCl_3 twice. The resulting resin was dried in vacuo.

4.10. Construction of a random DNA phage library

For the preparation of a duplex DNA library, oligonucleotide GGGGATCCGAATTCT(NNK)₁₅TGAAAGCTTCTCGAGGG (0.056 pM) and CCCTCGAGAAGCTTCA (0.56 pM) were mixed with Klenow

buffer, heated to 95 °C for 5 min and annealed by cooling the mixture to 37 °C. The single-stranded regions were converted to duplex DNA by continuing the incubation at 37 °C for 2 h in the presence of dNTPs (2.5 mM) and Klenow enzyme (0.5 mU/ μL). After the reaction, double-stranded DNA was recovered by EtOH precipitation. The recovered DNA was then digested separately with *Eco*RI and *Hind*III restriction enzymes and inserted into the T7select10-3b vector, according to the manufacturer's instructions. The primary titer of this T7 phage pool was 1.6×10^7 pfu/mL. For the screening procedure, the phage pool was amplified up to 1.7×10^{10} pfu/mL using *Escherichia coli* (BLT5615) as the host strain.

4.11. Procedure for the T7 random phage display screening using the PEGA-supported PFOS analogue

PEGA-supported PFOS analogue (**8**) and control resin (**9**) (5 mg each) were pre-equilibrated with buffer A (50 mM Tris–HCl (pH 8.0), 150 mM NaCl; 1 mL) at 4 °C. For the removal of resin-binding phage clones, the phage library (500 $\mu\text{L} \times 2$) was incubated with the control resin (60 μL each) for 2 h at room temperature. The resin was precipitated and the supernatant was used for screening. The supernatant (500 $\mu\text{L} \times 2$) was incubated with each resin (60 μL each) for 4 h at room temperature. A hole was made in the bottom of a tube, and the resin was then centrifuged at 3300g for 1 min to remove the phage solution. The resin was washed with buffer B (50 mM Tris–HCl (pH 8.0), 150 mM NaCl, 0.1% Tween20; 600 μL) 12 times. The bound phage particles were eluted by 20 min incubation with 1% SDS (100 μL). The eluted phage particles were amplified by infection into *E. coli* strain BLT5615 as host cells. The amplified phage was applied by subsequent rounds of biopanning. Four rounds of biopanning were performed.

4.12. Characterization of binding phage

After the fourth round of biopanning, the eluted phage particles were applied to Luria-Bertani plates containing 50 $\mu\text{g}/\text{mL}$ carbenicillin. Thirty-two clones were randomly selected from the plate and each clone was dissolved in phage extraction solution (20 mM Tris–HCl pH 8.0, 100 mM NaCl, 6 mM MgSO_4). Phage DNA carrying insert DNAs was amplified by PCR using forward primer (5'-TGCTAACTTCCAAGCGGACC-3') and reverse primer (5'-TTGCCAGAACTCCCAA-3'). The PCR product was purified with ExoSAP-IT (GE Healthcare) and used for cycle sequence PCR with a BigDye Terminator 3.1 Cycle Sequence Kit (Applied Biosystems). The resulting fragments were precipitated with ethanol. The purified PCR products were sequenced on an ABI PRISM 3100 Genetic Analyzer (Applied Biosystems). From the results, the deduced amino acid sequence present on the T7 phage capsid was determined.

4.13. Analysis of selected peptides using the Receptor Ligand Contacts (RELIC) bioinformatics

Peptide sequences obtained by phage DNA sequencing were analyzed using the RELIC program according to the supplier's manuals. The peptide sequences (PVSPTCDLGARTSP, VRDVFSVCGGVSSCH, LSRAGSLLGRSLRHA, SCTSYAGSLNFSL, LHSFDFVTNVSVFV, SCTSYVVGSLNFSL, PVLSPPPFDAGLVLK, SRFCNLGACPVRA, FGCTLP-IVACRVADE, GCLSTGYGPWWLPR) were used as a query for a FASTask search.³²

4.14. Surface plasmon resonance

A soluble form of recombinant CD14 that lacked the C-terminal 21 amino acids (sCD14 [1–335]) was purchased from ITSI-

Biosciences. Surface plasmon resonance (SPR) analysis was performed on a BIAcore 3000 (GE Healthcare). The surface of a CM5 chip was activated by injecting a solution containing 0.2 M *N*-ethyl-*N'*-(3-dimethylaminopropyl) carbodiimide hydrochloride and 50 mM *N*-hydroxysuccinimide for 10 min. Protein diluted with 10 mM sodium acetate buffer at pH 4.0–6.0 was injected and the surface was then blocked by injecting 1 M ethanolamine at pH 8.5 for 10 min. sCD14 protein was immobilized on the chip at a level of approximately 15,000 response units (RU). Perfluorooctanesulfonic acid (Wako Pure Chemical Industries, Ltd) at various concentrations (2.5, 5.0, 7.5, 10.0, 12.5, 15, 20, 25 and 30 μ M) in PBS (pH 7.4) were flowed at 20 μ L/min. To regenerate the sensor chip we used 25 mM NaOH and 0.5 mM NaCl and replicates of each experiment were performed more than two times. After the negative sensorgrams were mirrored, dissociation constant (K_D) response curves were generated by subtraction of the background signal generated simultaneously on the control flow cell. We used BIA evaluation 4.1 software (GE Healthcare) to determine the kinetic parameters.

4.15. Measurement of TNF- α level in the cell culture medium of mouse macrophages

A mouse macrophage cell line, RAW264.7, was obtained from the American Type Culture Collection (ATCC) (Manassas). The cells were cultured in Eagle's Minimum Essential Medium (MEM) supplemented with 4.5 g glucose per liter plus 10% fetal calf serum, 5 μ M L-glutamine, 50 units/mL penicillin and 50 units/mL streptomycin. The cells were cultured at 37 °C in standard medium in a humidified atmosphere of 5% CO₂–95% air. RAW264.7 cells were placed in a 12-well plate at 1×10^5 cells/well and incubated for 24 h. The various molecular ratios of CD14 protein and perfluorooctanesulfonic acid were pre-incubated for 10 min at room temperature, and these mixtures were added to the cell culture media. After stimulation with CD14 (final concentration of 10 μ M) for 24 h, the cell culture medium was collected to measure the amount of TNF- α secreted. The concentration of TNF- α in the culture medium was quantified by using a commercially available enzyme-linked immunosorbent assay (ELISA) development system (Bay Bioscience Co., Ltd) in accordance with the manufacturer's protocol.

Acknowledgments

This work was partially supported by Grant-in-Aid for Young Scientists (B) (22710219) (K.K.). We are grateful to Professor Akito Ishida (Kyoto Prefectural University) for valuable discussions on the SPR experiments.

References and notes

- European Food Safety Authority, *EFSA J.* **2008**, *653*, 1.
- Sohlenius, A. K.; Eriksson, A. M. *Pharmacol. Toxicol.* **1993**, *72*, 90.
- Shibley, J. M.; Hurst, C. H.; Tanaka, S. S.; DeRoos, F. L.; Butenhoff, J. L.; Seacat, A. M.; Waxman, D. J. *Toxicol. Sci.* **2004**, *80*, 151.
- van den Heuvel, J.; Thompson, J.; Frame, S.; Gillies, P. *Toxicol. Sci.* **2006**, *92*, 476.
- Abbott, B. D. *Reprod. Toxicol.* **2009**, *27*, 246.
- Lau, C.; Anitole, K.; Hodes, C.; Lai, D.; Pfahles-Hutchens, A.; Seed, J. *Toxicol. Sci.* **2007**, *99*, 366.
- Abbott, B. D.; Wolf, C. J.; Das, K. P.; Zehr, R. D.; Schmid, J. E.; Lindstrom, A. B.; Strynar, M. J.; Lau, C. *Reprod. Toxicol.* **2009**, *27*, 258.
- DeWitt, J. C.; Shnyra, A.; Badr, M. Z.; Loveless, S. E.; Hoban, D.; Frame, S. R.; Cunard, R.; Anderson, S. E.; Meade, B. J.; Peden-Adams, M. M.; Luebke, R. W.; Luster, M. I. *Crit. Rev. Toxicol.* **2009**, *39*, 76.
- Hallyathan, B.; Spydevold, O. *Biochim. Biophys. Acta* **1992**, *1128*, 65.
- Hu, W.; Jones, P. D.; Celius, T.; Giesy, J. P. *Environ. Toxicol. Pharmacol.* **2005**, *19*, 57.
- Luebker, D. J.; Hansen, K. J.; Bass, N. M.; Butenhoff, J. L.; Seacat, A. M. *Toxicology* **2002**, *176*, 175.
- Hu, W.; Jones, P. D.; Upham, B. L.; Trosko, J. E.; Lau, C.; Giesy, J. P. *Toxicol. Sci.* **2002**, *68*, 429.
- Hu, X. Z.; Hu, D. C. *Arch. Toxicol.* **2009**, *83*, 851.
- Qian, Y.; Ducatman, A.; Ward, R.; Leonard, S.; Bukowski, V.; Guo, N. L.; Shi, X.; Hallyathan, V.; Castranova, V. J. *Toxicol. Environ. Health A* **2010**, *73*, 819.
- Zhao, B.; Hu, G. X.; Chu, Y.; Jin, X.; Gong, S.; Akingbemi, B. T.; Zhang, Z.; Zirkin, B. R.; Ge, R. S. *Chem.-Biol. Interact.* **2010**, *188*, 38.
- Zhao, B.; Lian, Q.; Chu, Y.; Hardy, D. O.; Li, X. K.; Ge, R. S. *J. Steroid. Biochem.* **2011**, *125*, 143.
- Nakamura, R.; Takeuchi, R.; Kuramochi, K.; Mizushima, Y.; Ishimaru, C.; Takakusagi, Y.; Takemura, M.; Kobayashi, S.; Yoshida, H.; Sugawara, F.; Sakaguchi, K. *Org. Biomol. Chem.* **2007**, *5*, 3912.
- Smith, G. P.; Petrenko, V. A. *Chem. Rev.* **1997**, *97*, 391.
- Sche, P. P.; McKenzie, K. M.; White, J. D.; Austin, D. J. *Chem. Biol.* **1999**, *6*, 707.
- Jin, Y.; Yu, J.; Yu, Y. G. *Chem. Biol.* **2002**, *9*, 157.
- Shim, J. S.; Lee, J.; Park, H. J.; Park, S. J.; Kwon, H. J. *Chem. Biol.* **2004**, *11*, 1455.
- Makowski, L.; Rodi, D. J. *Hum. Genomics* **2004**, *1*, 41.
- Dorst, B. V.; Mehta, J.; Roush-Martin, E.; Coen, W. D.; Blust, R.; Robbens, J. *Toxicol. In Vitro* **2011**, *25*, 388.
- Rodi, D. J.; Jones, R. W.; Sangane, H.; Holton, R. A.; Wallace, B. A.; Makowski, L. *J. Mol. Biol.* **1999**, *285*, 197.
- Rodi, D. J.; Agoston, G. E.; Manon, R.; Lapcevic, R.; Green, S. J.; Makowski, L. *Comb. Chem. High Throughput Screening* **2001**, *4*, 553.
- Rodi, D. J.; Soares, A. S.; Makowski, L. *J. Mol. Biol.* **2004**, *322*, 1039.
- Mandava, S.; Makowski, L.; Devapalli, S.; Uzubell, J.; Rodi, D. J. *Proteomics* **2004**, *4*, 1439.
- Takakusagi, Y.; Kuramochi, K.; Takagi, M.; Kusayanagi, T.; Manita, D.; Ozawa, H.; Iwakiri, K.; Takakusagi, K.; Miyano, Y.; Nakazaki, A.; Kobayashi, S.; Sugawara, F.; Sakaguchi, K. *Bioorg. Med. Chem.* **2008**, *16*, 9837.
- Takakusagi, Y.; Takakusagi, K.; Sugawara, F.; Sakaguchi, K. *Expert Opin. Drug Disc.* **2010**, *5*, 361.
- Kuramochi, K.; Miyano, Y.; Enomoto, Y.; Takeuchi, R.; Ishi, K.; Takakusagi, Y.; Saitoh, T.; Fukudome, K.; Manita, D.; Takeda, Y.; Kobayashi, S.; Sakaguchi, K.; Sugawara, F. *Bioconjugate Chem.* **2008**, *19*, 2417.
- Meldal, M. *Tetrahedron Lett.* **1992**, *33*, 3077.
- Because the clone 3 does not have the inserted DNA fragment, the clone 3 peptide was excluded from the FASTAscan analysis. The clone 1, 4, 5, 6, 7, 9, 10, and 11 peptides as well as amino acid sequences of the first 15 residues of clone 2 and clone 8 peptides were used as a query for the FASTAscan analysis (see also Section 4.13.)
- Stelter, F.; Pfister, M.; Bernheiden, M.; Jack, R. S.; Bufler, P.; Engelmann, H.; Schütt, C. *Eur. J. Biochem.* **1996**, *236*, 457.
- Shin, H. J.; Lee, H.; Park, J. D.; Hyun, H. C.; Sohn, H. O.; Lee, D. W.; Kim, Y. S. *Mol. Cell* **2007**, *24*, 119.
- Gestwicki, J. E.; Hsieh, H. V.; Pitner, J. B. *Anal. Chem.* **2001**, *73*, 5732.
- Stokmaier, D.; Khorev, O.; Cutting, B.; Born, R.; Ricklin, D.; Ernst, T. O. G.; Böni, F.; Schwingruber, K.; Gentner, M.; Wittwer, M.; Spreafico, M.; Vedani, A.; Rabbani, S.; Schwarzt, O.; Ernst, B. *Bioorg. Med. Chem.* **2009**, *17*, 7254.
- Mesch, S.; Moser, D.; Strasser, D. S.; Kelm, A.; Cutting, B.; Rossato, G.; Vedani, A.; Koliwer-Brandl, H.; Wittwer, M.; Rabbani, S.; Schwarzt, O.; Kelm, S.; Ernst, B. *J. Med. Chem.* **2010**, *53*, 1597.
- Haziot, A.; Chen, S.; Ferrero, E.; Low, M. G.; Silber, R.; Goyert, S. M. *J. Immunol.* **1988**, *141*, 547.
- Hailman, E.; Lichenstein, H. S.; Wurfel, M. M.; Miller, D. S.; Johnson, D. A.; Kelley, M.; Busse, L. A.; Zukowski, M. M.; Wright, S. D. *J. Exp. Med.* **1994**, *179*, 269.
- Thomas, C. J.; Kapoor, M.; Sharma, S.; Bausinger, H.; Zyilan, U.; Lipsker, D.; Hanau, D.; Suroli, A. *FEBS Lett.* **2002**, *531*, 184.
- Hailman, E.; Vasselon, T.; Kelley, M.; Busse, L. A.; Hu, M. C.; Lichenstein, H. S.; Detmers, P. A.; Wright, S. J. *Immunol.* **1996**, *156*, 4384.
- DeWitt, J. C.; Peden-Adams, M. M.; Keller, J. M.; Germolec, D. R. *Toxicol. Pathol.* **2012**, *40*, 300.
- Brieger, A.; Bienefeld, N.; Hasan, R.; Goerlich, R.; Haase, H. *Toxicol. In Vitro* **2011**, *25*, 960.
- Corsini, E.; Avogadro, A.; Galbiati, V.; dell'Agli, M.; Marinovich, M.; Galli, C. L.; Germolec, D. R. *Toxicol. Appl. Pharmacol.* **2011**, *250*, 108.
- Corsini, E.; Sangiovanni, E.; Avogadro, A.; Galbiati, V.; Viviani, B.; Marinovich, M.; Galli, C. L.; Dell'Agli, M.; Germolec, D. R. *Toxicol. Appl. Pharmacol.* **2012**, *258*, 248.
- Kissa, E. *Fluorinated Surfactants and Repellents*; Marcel Dekker: New York, 2001.